Calcium-induced Inactivation of Alamethicin in Asymmetric Lipid Bilayers

JAMES E. HALL and MICHAEL D. CAHALAN

Department of Physiology and Biophysics, University of California, Irvine, California 92717

ABSTRACT This paper discusses a calcium-dependent inactivation of alamethicin-induced conductance in asymmetric lipid bilayers. The bilayers used were formed with one leaflet of phosphatidyl ethanolamine (PE) and one of phosphatidyl serine (PS). Calcium, initially confined to the neutral lipid (PE) side, can pass through the open alamethicin channel to the negative lipid (PS) side, where it can bind to the negative lipid and reduce the surface potential. Under appropriate circumstances, the voltage-dependent alamethicin conductance is thereby inactivated. We have formulated a model for this process based on the diffusion of calcium in the aqueous phases and we show that the model describes the kinetic properties of the alamethicin conductance under various circumstances. EGTA on the PS side of the membrane reduces the effects of calcium dramatically as predicted by the model.

INTRODUCTION

Calcium and other related divalent cations ions are implicated in several important physiological processes. They alter surface potentials near voltage-gated channels (Gilbert and Ehrenstein, 1969; Begenisich, 1975; Hille et al., 1975). Calcium is necessary for release of transmitter from nerve terminals (Kelly et al., 1979) and for secretion of hormone or cell product in certain secretory cells (Ginsberg and House, 1980). Calcium is an important part of the cyclic AMP control system (Berridge, 1975) and is involved in the process of vision (Hubbell and Bownds, 1979). A calcium-stimulated potassium current is found in many cells (Meech, 1978). Not all of the physiological effects of calcium are well understood, but it seems possible that some of these effects arise because calcium can bind to negative, membrane-bound phosphatidyl serine and the phosphatidyl inositides.

This paper explores the mechanism of calcium-induced inactivation of alamethicin conductance in asymmetric black lipid films. We are able to describe our results quantitatively by a detailed model, and the results suggest conditions under which similar calcium-controlled processes could be of physiological relevance. In the companion paper (Cahalan and Hall, 1982), we describe analogous results obtained in the node of Ranvier using alamethicin to induce conductance, apply the model presented in this paper to the

J. GEN. PHYSIOL. © The Rockefeller University Press · 0022-1295/82/03/0387/23 $1.00 387
Volume 79 March 1982 387-409

results, and find that the model's predictions describe the node data qualitatively.

MATERIALS AND METHODS

Most measurements reported here were performed on asymmetric lipid bilayers with one monolayer formed from bacterial phosphatidyl ethanolamine (PE) and one from bovine phosphatidyl serine (PS). Lipids from Supelco, Inc., Bellafonte, Pa. or Avanti Biochemicals, Inc., Birmingham, Ala. gave indistinguishable results. A few experiments used symmetric membranes made of mixtures of PE and PS. The method of membrane formation was similar to that originally described by Montal and Mueller (1972), but differed in some important details.

We used a truncated cone-shaped teflon chamber bisected along the axis of the cone into two halves machined as mirror images of each other (similar to a design of Schindler and Feher [1976]). A thin piece of teflon with a 0.012-in-Diam hole punched by a ground and sharpened No. 30 hypodermic needle was mounted between the two halves of the chamber, using a minimum of silicon vacuum grease to insure a good seal. The two halves of the chamber were then forced into a tapered hole in a square aluminum block. This served to clamp the two halves of the chamber together and to provide an isothermal enclosure for the chamber, whose temperature was controlled by a feedback circuit using a thermistor in contact with the aluminum block and two Peltier thermo-electric elements attached on either side of the block.

Membranes were formed by filling each half of the chamber with 2.0–3.0 ml of aqueous solution and then withdrawing enough of the solution from each chamber to lower the levels of the solution to 5–10 mm below the hole in the thin teflon partition. This was accomplished using 1-ml tuberculin syringes inserted in vertical holes starting at the top of each chamber half and opening near the bottom. A small drop of squalene (2–5 μl) purified by passage through an alumina column was then placed in the hole using a glass microliter pipette. Lipid solution (10 mg/ml lipid in pentane) was then added to the front and back chambers using glass microliter pipettes. An attempt was made to deliver the pentane-lipid mixture as close to the intersection of the water surface and teflon chamber wall as possible. The monolayers of lipid were then raised by injecting previously withdrawn water from the tuberculin syringes into the chambers.

Membrane formation was monitored by observing the current response to a 10-mV amplitude triangular voltage, the amplitude of the current square wave being proportional to the capacitance. The membranes thus formed had a specific capacitance of $\sim 0.8\ \mu F/cm^2$, and an area of $\sim 7 \times 10^{-4}\ cm^2$.

Current-voltage curves were measured using a four-electrode system. Electrodes were chlorided 12-gauge silver wire. Current was measured with an AD 42K operational amplifier (Analog Devices, Inc., Norwood, Mass.) in a virtual ground configuration, and voltage was measured with an electrometer amplifier using AD523 (Analog Devices, Inc.) op-amps as voltage followers. Voltage pulses were generated either by a computer controlled 12-bit DAC (digital-to-analog converter) (AD 5782, Analog Devices, Inc.) buffered by an op-amp (AD 514, Analog Devices, Inc.) or by a battery-driven potentiometer. Voltage ramps for current-voltage curves were always generated by computer-controlled DAC. Current-voltage curves were recorded on an X-Y recorder (HP 7034A, Hewlett-Packard Co., Palo Alto, Calif.) and current-time curves at constant voltage were recorded on the same recorder with an X-axis timebase. Alamethicin used in these experiments was obtained from Dr. G. B. Whitfield of the Upjohn Company, Kalamazoo, Mich. and used without further purification.

Nonactin isolated from *Streptococcus aureus* was purchased from Sigma Chemical Co., St. Louis, Mo. Salts used in solution preparation were reagent grade purchased from Mallinckrodt Inc., St. Louis, Mo.

The membrane preparation used in all the experiments reported here was one in which PE formed one leaflet of the bilayer and PS formed the other. The solution bathing both sides of the membrane was initially 0.1 M KCl buffered at pH 7 with 5 mM Hepes in all cases reported here. Alamethicin was added to either the PE side of the membrane or to both sides in equal concentrations. By convention, the PS side or the side opposite the addition of alamethicin is ground. Before addition of alamethicin, the asymmetry potential of the membrane was estimated using the asymmetry of the nonactin-K^+ current-voltage curve (Hall and Latorre, 1976; Hall, 1981). Even after the addition of alamethicin, reliable values of asymmetry potential can be obtained by sweeping rapidly so that the alamethicin conductance does not have time to turn on. The values of asymmetry potential estimated from the nonactin-K^+ *I-V* curve are probably accurate to ~10–15 mV with reservations to be noted later.

After preparing the membrane and using nonactin to determine the surface potentials, the kinetics and steady-state characteristics of the alamethicin conductance were measured.

QUANTITATIVE MODEL

In this section, we develop a quantitative model for the interaction of alamethicin-induced conductance, diffusion of calcium in the unstirred layers, and the binding of calcium to a negatively charged membrane component.

Basic Properties of Alamethicin

Alamethicin is a voltage-dependent pore-former whose characteristics have been extensively studied by a number of workers (Eisenberg et al., 1973; Boheim, 1974; Gordon and Haydon, 1972). It allows the passage of both cations and anions and has an appreciable calcium conductance (Eisenberg et al., 1973). The steady-state conductance, G, depends exponentially on applied voltage, V:

$$G = G_o e^{V/V_o} = N_o \bar{\gamma} e^{V/V_o}$$

where G_o is the zero-voltage conductance, V_o is the voltage change that results in an e-fold change in conductance, and N_o is the number of pores open at 0 V. $\bar{\gamma}$ is the average conductance of a single pore, obtained by measurement of the conductances and lifetimes of the individual levels of a single pore (Eisenberg et al., 1973; Boheim, 1974).

On the application of a voltage pulse, the alamethicin conductance increases with time in a manner approximately described by a first-order linear differential equation:

$$\begin{aligned} \frac{dn}{dt} &= \mu(V) - n\lambda(V) \\ \mu(V) &= \mu_o \exp(V/V_\mu) \\ \lambda(V) &= \lambda_o \exp(-V/V_\lambda). \end{aligned} \tag{2}$$

With the voltage zero at time zero, the solution to this equation is:

$$n(t) = \frac{\mu}{\lambda}\{\exp(-\lambda(V)t)\} \tag{3}$$

Note that Eq. 2 and 3 show that the time constant, $\tau = 1/\lambda(V)$, for the development of the alamethicin conductance is voltage dependent, as is the initial rate of channel formation, $\mu(V)$.

An asymmetrical membrane with PE on one side and PS on the other has a bias electric field across the membrane that tends to turn on the conductance due to alamethicin on the PE side of the membrane. The current-voltage curve for a given alamethicin concentration is thus shifted to lower applied voltages by the electric field across the membrane. Eq. 1 thus becomes

$$G = G_o \exp\{(V - \phi)/V_o\} \tag{4}$$

where ϕ is the surface potential resulting from the negative charge of the PS.

The magnitude of ϕ is a function of the surface charge density, the concentration of monovalent ions, and the concentration of divalent ions. Divalents have a more dramatic effect than monovalents on the surface potential, a fact of possibly great physiological significance. If divalent ions are added to only one side of the membrane, the permeability of the membrane to divalents will be a major factor controlling their concentration on the other side. We consider here the case of divalents added to the side of the membrane opposite the negative charge (to the PE side) and allowed access to the PS side only through open alamethicin channels.

The alamethicin conductance, calcium concentration at the PS head groups, and surface potential thus all influence each other. Our task is to describe quantitatively their interrelations.

Assumptions

We will assume that the surface potential can be accurately described by the Gouy-Chapman theory with given surface charge (Bockris and Reddy, 1970):

$$\sinh(F\phi_o/2RT) = \frac{\sigma}{\sqrt{8RT\epsilon\epsilon_o\zeta}} \tag{5}$$

where ϕ_o is the surface potential, σ is the surface charge, R is the universal gas constant, T is the temperature, ϵ is the dielectric constant, ϵ_o is the permittivity of free space, and ζ is the ionic strength.[1] (The sign of ϕ is the same as that of σ).

Strictly speaking, to calculate the surface potential in the presence of a mixture of mono- and divalent ions, we should use the Grahame equation

[1] A convenient numerical form of this equation is given by McLaughlin et al. (1970):

$$\sinh(F\phi_o/2RT) = 136\sigma/\sqrt{\xi},$$

where the temperature is 20°C, the dielectric constant of water is used, σ is in electronic charges per square angstrom, and ξ is in moles per liter.

instead of the Gouy equation. But because the concentration of calcium ions on the side of the membrane of interest is so low compared with the monovalent concentration, the two equations give essentially identical results. The small correction of using ionic strength, ζ, instead of monovalent concentration alone, extends the range of agreement to higher calcium concentrations.

We also assume the effective surface charge can be determined from the density of negatively charged lipid head groups by an adsorption isotherm for divalent ions. We will argue later that this assumption, certainly not true at high divalent ion concentrations, is probably valid under our experimental conditions. Thus

$$\sigma = \sigma_o \frac{(1 - K_M M_o^{++})}{(1 + K_M M_o^{++})} \tag{6}$$

where σ is the effective surface charge, σ_o in the density of negatively charged lipids, M_o^{++} is the concentration of divalent ions *near the membrane surface*, and K_M is the binding constant for M^{++} to the negative lipid.

Divalent movement in the aqueous phases is described by the diffusion equation:

$$\frac{dM^{++}}{dt} = D \frac{d^2M^{++}}{dx^2} \tag{7}$$

where D is the divalent ion's diffusion coefficient.

In steady state, $dM^{++}/dt = 0$, and the divalent flux density is given by

$$\Psi = -D \frac{dM^{++}}{dx} \tag{8}$$

where Ψ is the flux in moles per meter squared per second.

We will use the unstirred-layer approximation to Eq. 8. Here it is assumed that stirring or convection completely and rapidly mix the solutions up to a distance δ away from the membrane. Closer to the membrane than δ, transport is diffusion controlled. Thus Eq. 8 has the solution

$$\Psi = \frac{D\Delta M^{++}}{\delta} \tag{9}$$

where ΔM^{++} is the difference between the concentration of M^{++} in bulk and that at the membrane.

Steady-State Treatment

We first calculate the interaction between the alamethicin conductance, the flux of calcium, and the surface potential in steady state. We will use the assumptions stated above and treat the case where alamethicin and divalent ions are added to the same side of the membrane. That side of the membrane is considered neutral and the side opposite is considered to have a negative charge. Fig. 1 shows schematically the essentials of the steady-state treatment. Fig. 1 B shows how increasing the permeability of the membrane to calcium

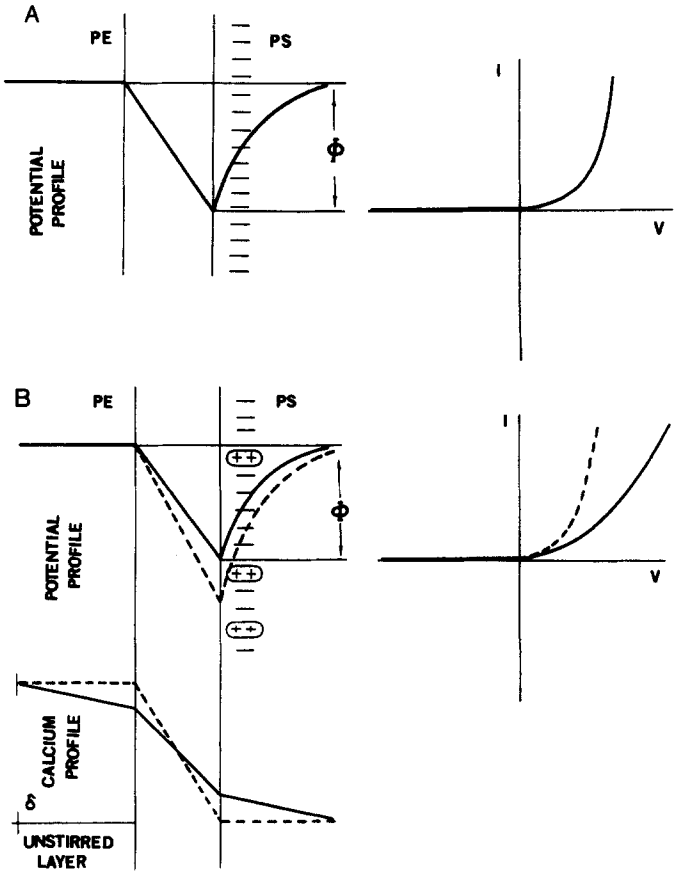

FIGURE 1. Schematic drawing of how calcium on the PE side flattens the alamethicin current-voltage curve. (A) surface potential at zero applied volts and *I-V* curve with no calcium in either compartment; (B) surface potential profile and the calcium profile with (solid line) and without (dotted line) the alamethicin conductance turned on. When the alamethicin conductance is off, the membrane is impermeant to calcium and the surface concentration of calcium is the same as that a long distance from the membrane. When the alamethicin conductance is turned on, the membrane becomes highly permeable to calcium and the concentration of calcium increases on the PS side and decreases on the PE side.

alters the calcium concentration at the membrane surfaces and reduces the surface potential.

In steady state, the flux of divalent ions through the unstirred layers and the flux through the membrane $J_{M^{++}}$ must be equal.

Thus,

$$J_{M^{++}} = \frac{FDM_o^{++}}{\delta} \tag{10}$$

where M_o^{++} is the concentration of divalent ion far enough from the negatively charged surface to be uninfluenced by the surface potential, i.e., several Debye lengths from the membrane surface. Eq. 10 is written for the PS side of the membrane, the side on which the calcium concentration very far from the membrane is zero, but in steady state it is valid everywhere. Since the Debye length is only ~1 nm and the unstirred layer is ~100 μm, the error made in Eq. 11 by this approximation is negligible.

To obtain an analytically tractable expression for the surface potential, we expand the surface potential in a Taylor series about the initial value of the surface charge with no divalent on the negatively charged side of the membrane:

$$\phi(\sigma) = \phi(\sigma_o) + 2 \tanh\left(\frac{F\phi_o}{2RT}\right)\frac{RT}{F}\frac{\Delta\sigma}{\sigma_o} + O(\Delta\sigma)^2. \tag{11}$$

Eq. 6 gives $\Delta\phi$ in terms of M_o^{++}, and Eq. 11 becomes

$$\Delta\phi = \frac{4\,RT}{F}\tanh\left(\frac{F\phi_o}{RT}\right)\left[\frac{K_M M_o^{++}}{1 + K_M M_o^{++}}\right] = \psi_o\left[\frac{K_M M_o^{++}}{1 + K_M M_o^{++}}\right] \tag{12}$$

where the definition of ψ_o is expressed by the first line of Eq. 12.

Solving for M_o^{++} gives

$$M_o^{++} = \frac{1}{K_M}\frac{\Delta\phi}{\psi_o - \Delta\phi}. \tag{13}$$

We want a relation between the conductance in the absence of divalent ions and that after divalents are added. This is

$$G_{M^{++}} = G_o \exp\{(V - (\phi_o + \Delta\phi))/V_o\} = G_{co}\exp\{-\Delta\phi/V_o\}. \tag{14}$$

$G_{M^{++}}$ is the total conductance as a function of voltage in the presence of divalent ion, $\Delta\phi$ is the shift in surface potential due to the divalent, ϕ_o is the surface potential in the absence of the divalent, ϕ_o is the surface potential in the absence of the divalent, and G_{co} is the control conductance as a function of voltage with ϕ_o surface potential. The flux of divalents can thus be calculated as

$$J_{M^{++}} = \frac{\bar{\gamma}_{M^{++}}}{\bar{\gamma}_{M^{++}} + \bar{\gamma}_o}(V - E_{M^{++}})G_{M^{++}} \tag{15}$$

where $\bar{\gamma}_{M^{++}}$ is the mean alamethicin single-channel conductance to divalent cation ion only, $\bar{\gamma}_o$ is the mean single-channel conductance in the absence of divalent, and $E_{M^{++}}$ is the reversal potential for the divalent cation ion. Eq. 15 expresses the assumption that divalent and monovalent ions do not interfere with each other in the alamethicin channel. This assumption is probably a good one, since the alamethicin channel is large and has a conductance proportional to the conductance of the bulk solution bathing the membrane for a wide variety of conditions (Eisenberg et al., 1973). To estimate $\bar{\gamma}_{M^{++}}$, a value too small to be measured directly, we used the single-channel conduct-

ance in 1 M $CaCl_2$, corrected for the chloride conductance using the reversal potential in asymmetric solutions, and scaled the conductance with the average calcium concentration on the two sides of the membrane. $E_{M^{++}}$ is strictly infinite with zero calcium on one side of the membrane. This situation clearly never exists, and as a practical matter, we assumed the calcium concentration on the PS side of the membrane was never greater than 10^{-6} M, a value consistent with the expected calcium contamination in the reagent grade salts we used. Equating the values of $J_{M^{++}}$ given by Eqs. 10 and 15 using the value of $M_{o^{++}}$ given by Eq. 13 gives

$$(V - E_{M^{++}}) \frac{\bar{\gamma}_{M^{++}}}{\bar{\gamma} + \bar{\gamma}_o} G_{M^{++}} = \frac{FD}{\delta K_M} \frac{\Delta\psi}{\chi_o - \Delta\phi}. \tag{16}$$

Solving for $\Delta\phi$ under the assumption $\Delta\phi \ll \psi_o$, almost certainly true, gives

$$\Delta\phi = \psi_o \frac{\delta K_M}{FD} \frac{\bar{\gamma}_{M^{++}}}{\bar{\gamma}_{M^{++}} + \bar{\gamma}_o} (V - E_{M^{++}}) G_{M^{++}}. \tag{17}$$

This expression says that the surface potential shifts by an amount proportional to the conductance from the value it would have in the absence of divalent ions. The larger the conductance, the larger the shift.

From Eq. 14, the logarithmic derivative of $G_{M^{++}}$ with voltage is

$$\frac{d \ln G_{M^{++}}}{dV} = \frac{1}{V_o} + \frac{1}{V_o} \frac{d\Delta\phi}{dG_{M^{++}}} \frac{d \ln G_{M^{++}}}{dV} G_{M^{++}}. \tag{18}$$

Solving for $\frac{d \ln G_{M^{++}}}{dV}$ gives

$$\frac{1}{\left\{\frac{d \ln G_{M^{++}}}{dV}\right\}} = V_o + \frac{\left\{\frac{\psi_o \delta K_M \bar{\gamma}_{M^{++}} (V - E_{M^{++}}) G_{M^{++}}}{FD(\bar{\gamma}_{M^{++}} + \bar{\gamma}_o)}\right\}}{\left\{1 - \frac{\psi_o \delta K_M \bar{\gamma}_{M^{++}}}{FD(\bar{\gamma}_{M^{++}} + \bar{\gamma}_o)} G_{M^{++}}\right\}} \tag{19}$$

Expanding the denominator, assuming the second term is nearly zero, gives

$$\frac{1}{\left\{\frac{d \ln G_{M^{++}}}{dV}\right\}} = V_o + \left\{\frac{\psi_o \delta K_M \bar{\gamma}_{M^{++}} (V - E_{M^{++}})}{FD(\bar{\gamma}_{M^{++}} + \bar{\gamma}_o)}\right\} G_{M^{++}}. \tag{20}$$

This is a very useful result because it provides a relationship between $1/(d \ln G_{M^{++}}/dV)$ and $G_{M^{++}}$, experimentally accessible quantities, and it can be used to estimate the binding constant, K_M, of divalent ion to negative lipid. Physically, Eq. 20 says that the higher the conductance, the less rapidly the conductance will change with increasing voltage, because the more calcium will be available to screen the surface potential and thus counteract the effect of applied voltage.

Time-dependent Treatment

We want to calculate the time dependence of the alamethicin conductance, the divalent ion conductance, and the surface potential upon the application of a voltage pulse. This requires the simultaneous solution of Eqs. 2 and 7 using Eqs. 5 and 6 to relate the divalent concentration and the surface potential. We have used an iterative computer program to generate a solution for the alamethicin conductance, divalent ion concentration, and surface potential as functions of time. The program breaks the unstirred layer into a number of planes of equal thickness and the time axis into uniform finite intervals. The initial value of the alamethicin conductance, usually zero, is prescribed and the rate of change of the conductance is calculated from Eq. 2. The value of the divalent flux across the membrane is calculated from Eq. 15 using the value of $G_{M^{++}}$. This value is used to determine dM^{++}/dx at the surface of the membrane. New divalent concentrations at each plane of the unstirred layer are then calculated. The value of divalent concentration at the most distant plane from the membrane on the neutral lipid side is the bulk value and at the corresponding plane on the other side it is zero.

The divalent concentration near the membrane (but far enough away not to be influenced by the surface potential) is multiplied by $\exp(2F\phi_o/RT)$ where ϕ_o is the surface potential at the previous iteration, and is used in Eq. 6 to calculate the new value of the surface potential. This is then used to calculate the new effective voltage across the membrane. The new conductance is determined by using Eq. 2 as a finite difference approximation. The whole process is then iterated repeatedly to generate a solution for the desired time period.

The program, written in Fortran, requires as inputs the initial surface charge, the bulk divalent ion concentration on the neutral side, the alamethicin conductance parameters, the diffusion coefficients of the divalent ion on both sides of the membrane, and the binding constant of divalent to negative lipid. Comparison of computer-generated solutions and experimental results will be made at appropriate points.

The essential result of computer simulation is that alamethicin conductance will exhibit inactivation resulting from the binding of divalent ions to the negative charge and consequent alteration of the electric field across the membrane.

Recovery from Inactivation

Recovery from inactivation can also be simulated by the computer program. But because the alamethicin conductance is zero during essentially all of the recovery phase, its time-course is determined entirely by diffusion in the unstirred layer. An analytical solution of the diffusion equation with appropriate boundary conditions (Mathews and Walker, 1965) in the unstirred layer gives

$$M^{++}(x,t) = \frac{2M_o^{++}}{\pi^{3/2}} \sum_{n=0}^{\infty} \left\{ \frac{\cos\{(n+\tfrac{1}{2})\pi x/\delta\}}{(n+\tfrac{1}{2})^2} \exp\left(-(n+\tfrac{1}{2})^2 \pi^2 \frac{Dt}{\delta^2} \right) \right\}. \quad (21)$$

This result shows that recovery from inactivation should take place exponentially with a time constant proportional to the square of the unstirred layer thickness.

Computer simulation shows that the peak amplitude of the inactivation recovery in a double pulse experiment (cf. Fig. 9 A and B) with variable time delay between pulses has the same time constant as the lower-order term in Eq. 21. Thus, the time-course of recovery from inactivation provides an estimate of unstirred layer thickness.

RESULTS

Both Alamethicin and Nonactin See the Same Surface Potential Difference

Because of lipid mixing before membrane formation, the difference in surface potential across asymmetric PS-PE membranes can vary by ~50 mV if special care is not taken. Asymmetric membranes with low surface potential difference as detected by the nonactin $-K^+$ *I-V* curve tend to show a very high zero-volt nonactin conductance. This argues that the major cause of reduction of asymmetry is transfer of PS to the PE side, increasing the negative surface charge density on the PE side. In cases where asymmetry less than the expected value of ~100 mV is initially obtained, formation of a new membrane, after adding an additional 10 μl of PE-pentane mixture to the surface of the chamber initially containing PE, usually results in the expected 100 mV or greater asymmetry.

We took advantage of the occasional variability of membrane asymmetry to determine the correlation between surface potential and the voltage at which the alamethicin conductance reached a value of 70 $\mu S/cm^2$. In these experiments, the alamethicin concentration in the PE compartment was always 2×10^{-7} g/ml. The alamethicin concentration in the PS compartment was either 0 or 2×10^{-7} g/ml. The amount of alamethicin in the PS compartment did not alter the position of the branch of the alamethicin current-voltage curve obtained when the voltage in the PE compartment was positive with respect to that in the PS compartment.

The alamethicin current-voltage curve is shifted by a voltage equal to the surface potential deduced by nonactin. Fig. 2 shows the voltage at which the alamethicin conductance reaches 70 $\mu S/cm^2$ plotted against the nonactin-K^+ deduced surface potential. The correlation shows that the alamethicin current-voltage is shifted by the same amount as the surface potential change recorded by the nonactin *I-V* curve.

This verifies the expected dependence of alamethicin conductance on the electric field across the membrane, as described in Eq. 4, and allows us to replace the voltage, V, in all equations describing alamethicin conductance with $V_{app} + \phi_o$, where V_{app} is the applied voltage as measured by the voltmeter and ϕ_o is the measured surface potential.

We performed two kinds of control experiments in symmetric membranes. First, in PE membranes we found that asymmetric addition of calcium did not shift either the nonactin-K^+ *I-V* curve or the alamethicin current-voltage

curve. In the alamethicin experiments, calcium was added to the same side of the membrane as alamethicin and up to a concentration of 20 mM no shift was seen.

We also demonstrated that 20 mM calcium shifted both the alamethicin *I-V* curve and the nonactin current-voltage curve by ~40 mV in membranes made from a mixture of PE and PS (1:1 by weight). This result generalizes our assertion that alamethicin and nonactin see the same surface potential difference.

In the following sections, we will be concerned with the ways in which calcium can alter ϕ_o, and thus the electric field across the membrane, with no change in applied voltage.

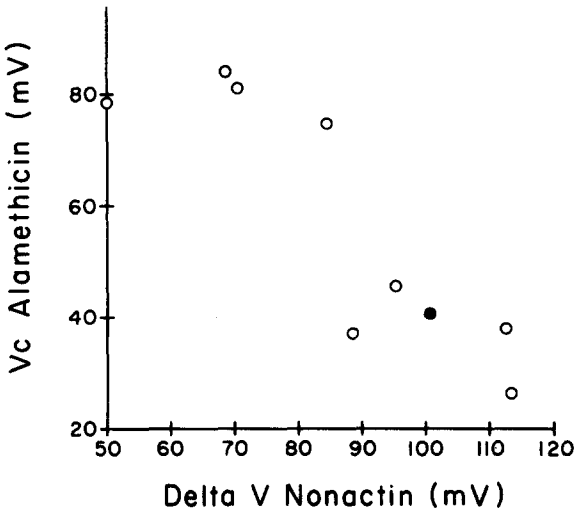

FIGURE 2. Surface potential difference between the PS and PE side of an asymmetric membrane (ΔV) as detected by the nonactin-K^+ current-voltage curve plotted against voltage at which the alamethicin conductance in the same membrane reaches a value of 70 $\mu S/cm^2$. The alamethicin concentration is always 2×10^{-7} g/ml on the PE side and except for the point marked (●) is the same on the PS side.

Calcium on the PE Side Flattens the Alamethicin Current-Voltage Curve

Fig. 3 A shows two current-voltage curves. Curve *i* was taken in the absence of calcium. On the addition of calcium to the PE side of the membranes, shown by curve *ii* in Fig. 3 A, the alamethicin current-voltage curve becomes much less steep, as predicted by Eq. 20. This result was intriguing because we had previously found that the alamethicin *I-V* curve in node of Ranvier is less steep than that in symmetric planar bilayers made of PE (Cahalan and Hall, 1979; Cahalan and Hall, 1982). Since the calcium concentration outside of the node is much higher than that inside, it seemed possible that the flatness of the alamethicin *I-V* curve in node might be explicable in terms of the

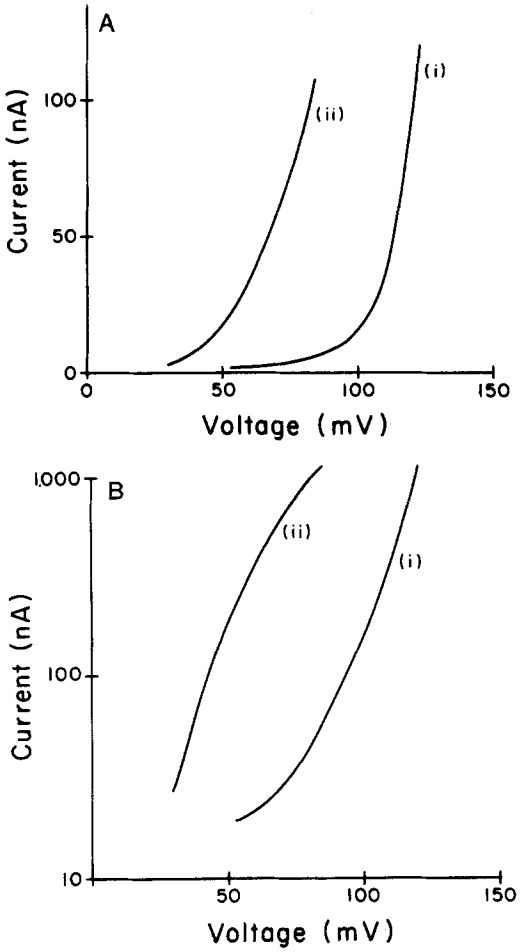

FIGURE 3. Steady-state current-voltage curves in asymmetric PE-PS membranes with alamethicin added to the PE side. By convention, the PS side is ground. The steeper curve (*i*) was obtained in the absence of calcium, the flatter curve (*ii*) in the presence of 20 mM calcium on the PE side of the membrane. In B, these data are shown on a logarithmic plot. Note that the slope of the flatter curve (with calcium) decreases progressively as the conductance is increased.

asymmetric calcium concentration rather than by an intrinsic property of nodal membrane.

Eq. 20 predicts that the logarithmic slope of the current-voltage curve should flatten progressively at higher conductances. Fig. 3 B shows logarithmic current-voltage curves without (curve *i*) and with (curve *ii*) calcium. Curve *ii* shows progressive flattening as expected.

The rate of flattening can be used to estimate the binding constant. Table

I shows a numerical differentiation of the conductance-voltage curve in Fig. 3 B. Plotting $1/\frac{\Delta \ln G}{\Delta V}$ against G in Siemens per centimeter squared gives a straight line with slope 16.8 V/(S/cm^2), as shown in Fig. 4.

We can use Eq. 20 and this value of the slope to estimate the apparent

TABLE I

V	G	ln G	Δln G	$\frac{\Delta V}{\Delta \ln G}$
mV	*nS*			$V \times 10^{-2}$
30	100	4.60	—	—
35	143	4.962	0.35	1.43
40	200	5.298	0.33	1.52
45	267	5.587	0.289	1.73
50	360	5.886	0.298	1.68
55	455	6.120	0.234	2.14
60	550	6.310	0.189	2.65
65	677	6.517	0.207	2.42
70	814	6.702	0.184	2.71
75	960	6.867	0.165	3.03
80	1100	7.003	0.136	3.60

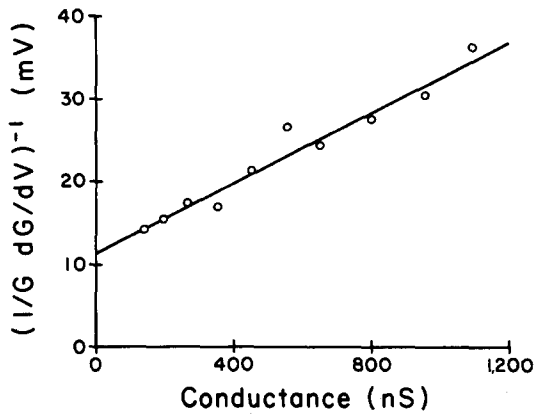

FIGURE 4. Plot of $1/(d\ln G/dV)$ vs. G. Our model predicts this curve should be a straight line with a slope related to the binding constant of calcium to phosphatidyl serine. The slope of the straight line is 2.4 × 10^4 V/S. The area of the membrane was 7 × 10^{-4} cm^2; thus the slope appropriate to Eq. 20 is 16.8 V/(S/cm^2).

binding constant of calcium to phosphatidyl serine. We use the following values: F = 96,500 coul/equivalent; $D = 5 \times 10^{-6}$ cm^2/s; $\delta = 10^{-2}$ cm^2; and ψ_o = 0.1 V, which is estimated from the nonactin-K$^+$ I-V curve asymmetry. The remaining values are slightly more controversial. We assume that $\bar{\gamma}_{M^{++}}$ and $\bar{\gamma}_o$ are proportional to the appropriate ionic concentrations. The ionic concentration appropriate to determine $\bar{\gamma}_{M^{++}}$ is the average of the calcium

concentrations on the two sides of the membrane just outside the diffuse double layer. For 100 mM KCl and 20 mM $CaCl_2$ on the PE side of the membrane, $\bar{\gamma}_{M^{++}}/\bar{\gamma}_o = 0.1$. This estimate of $\bar{\gamma}_{M^{++}}$ is probably accurate to 10%, judging from the behavior of single channel conductances under a wide variety of conditions (Eisenberg et al., 1973). Estimation of $(V - E_{M^{++}})$ is more uncertain because both V and $E_{M^{++}}$ are varying continuously along the curves in such a way as to reduce the curves' slope. Nevertheless, computer simulations show that the change is not too drastic because as V increases, $E_{M^{++}}$ becomes less negative so that their difference remains fairly constant. We therefore feel justified in using a value of ~100 mV for $(V - E_{M^{++}})$.

Using these values and equating the value of the slope (16.8 V/(S/cm^2) to the bracketed expression in Eq. 20 gives the value

$$K_{app} = 900\ M^{-1}$$

for the *apparent* binding constant. Correcting for the 75-mV surface potential deduced from the nonactin I-V curve,

$$K_{Ca^{++}} = K_{app} \exp(-2F\phi_o/RT)$$
$$= 2.2\ M^{-1}$$

Since we have probably overestimated the value of $(V - E_{M^{++}})$, this value is an underestimate of the value of $K_{Ca^{++}}$. It is nevertheless in reasonable agreement with the value of 12 M^{-1} reported by McLaughlin et al. (1981), particularly since we have had to estimate the calcium equilibrium, potential.

We conclude that flattening of the steady-state I-V curve in the presence of asymmetric calcium can be accounted for quantitatively by passage of calcium through the membrane and its subsequent binding to phosphatidyl serine.

Divalent Ions Produce Inactivation of the Alamethicin Conductance

The experiments described to this point all involve slow voltage changes so that steady-state conditions were achieved. But both alamethicin conductance and the calcium concentration of the PS side of the membrane can change with time after the application of a voltage pulse, and the time-course of each affects the time-course of the other.

In the absence of calcium on the PE side of the membrane, alamethicin kinetics in asymmetric PE-PS membranes are similar to those in symmetric PE-PE membranes. Application of a series of voltage pulses in the absence of calcium thus gives current vs. time curves like those shown in Fig. 5 A. The

FIGURE 5. (*opposite*) Response of the alamethicin current to a series of voltage pulses in the absence of calcium on either side of the membrane (A). When calcium is added to the PE side of the membrane (B), significant inactivation occurs at voltage and current levels similar to those where none occurs in the absence of calcium. This result shows that there is a *calcium-dependent* inactivation distinct from the inactivation that arises from phospholipid flip-flop (Hall, 1981). (Current levels are higher than for the control at similar voltages because negative surface charge on the PE side is reduced by addition of calcium.)

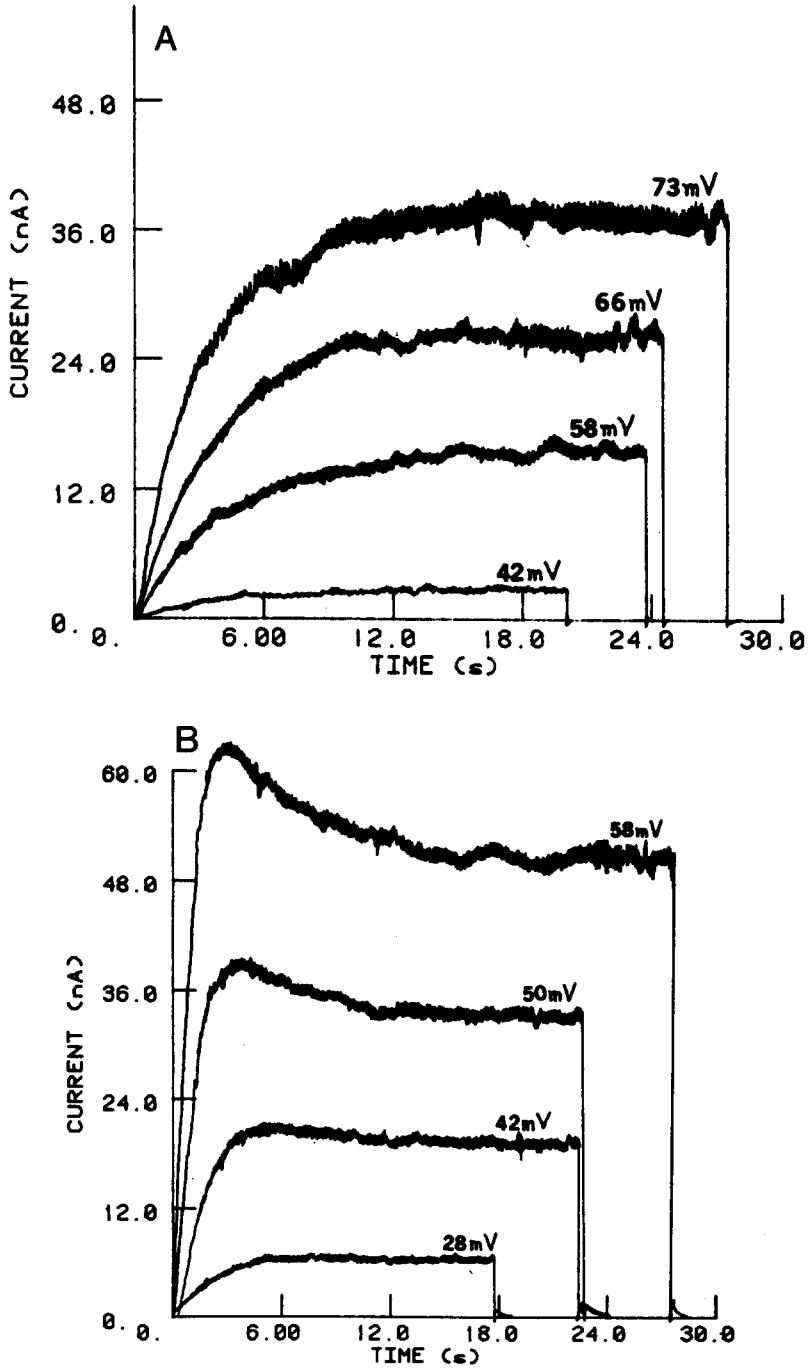
A
48.0
36.0
24.0
12.0
0. 0.
CURRENT (nA)
73mV
66mV
58mV
42mV
6.00
12.0
18.0
24.0
30.0
TIME (s)
B
60.0
48.0
36.0
24.0
12.0
0. 0.
CURRENT (nA)
58mV
50mV
42mV
28mV
6.00
12.0
18.0
24.0
30.0
TIME (s)

addition of calcium at 12.5 mM to the PE side produces curves like those in Fig. 5 B, which show pronounced inactivation. The current in the presence of calcium is higher than in the control case because a contaminating negative charge on the PE side is reduced by addition of calcium. This shifts the alamethicin *I-V* curve to lower voltages (cf. Fig. 3 A and B).

EGTA on the PS Side Reduces Inactivation

Addition of EGTA to the PS side of the membrane dramatically reduces the inactivation. Fig. 6 A shows inactivation in a membrane with a 135-mV surface potential at 58 and 43 mV applied voltage pulses. The current level here reached a maximum amplitude of 0.18 mA/cm^2. (Membrane current was actually ~100 nA.)

Immediately after these pulses, EGTA previously adjusted with KOH to pH 7.4 was added to the PS side to a concentration of 0.4 mM. Fig. 6 B shows the series of voltage pulses taken after this addition.

The inactivation is strikingly reduced at 40 mV and the steady-state current level is much higher than before the EGTA addition. Furthermore, the voltage dependence of the steady-state current has increased considerably. Whereas in Fig. 6 A, a 15-mV increase in voltage barely doubles the steady-state current, a 5-mV increase in voltage doubles the current in the presence of EGTA, as shown in Fig. 6 B.

These effects are exactly as expected from our model for the action of calcium. The model shows that the change in calcium concentration far from the membrane necessary to produce these effects is very small, <0.1 mM, and even though the EGTA concentration is small, it still reduces the value of the calcium concentration by a large factor and thus decreases its effects dramatically.

The binding constant for calcium to PS is ~12 M^{-1}(McLaughlin et al., 1980), but the apparent binding constant at low calcium concentrations is much higher because of the surface potential due to the PS.

The Surface Charge Model Describes the Observed Kinetics

Fig. 7 shows a comparison of the experimental current response to a 58-mV voltage pulse with the current response of the model. The parameters of the model were chosen by using the measured value of the surface potential to estimate an effective surface charge and a 100-μm unstirred layer thickness. The calcium diffusion coefficient was taken as 5×10^{-6} cm^2/s, a mean of the value in various concentration aqueous solutions. The values of V_λ and V_μ

FIGURE 6. (*opposite*) Inactivation of alamethicin in the presence of 10 mM calcium for three voltage pulses. The surface potential difference from nonactin is ϕ_0 = 135 mV. The alamethicin concentration is 2×10^{-7} g/ml in 0.1 M KCl buffered to pH 7.0 with 5 mM Hepes (A). The results in B were obtained with 0.4 mM EGTA on the PS side of the membrane. EGTA shifts the alamethicin *I-V* curve to lower voltages (by removing contaminating divalents) and protects against inactivation at current levels and voltage levels similar to those where inactivation readily occurs in its absence.

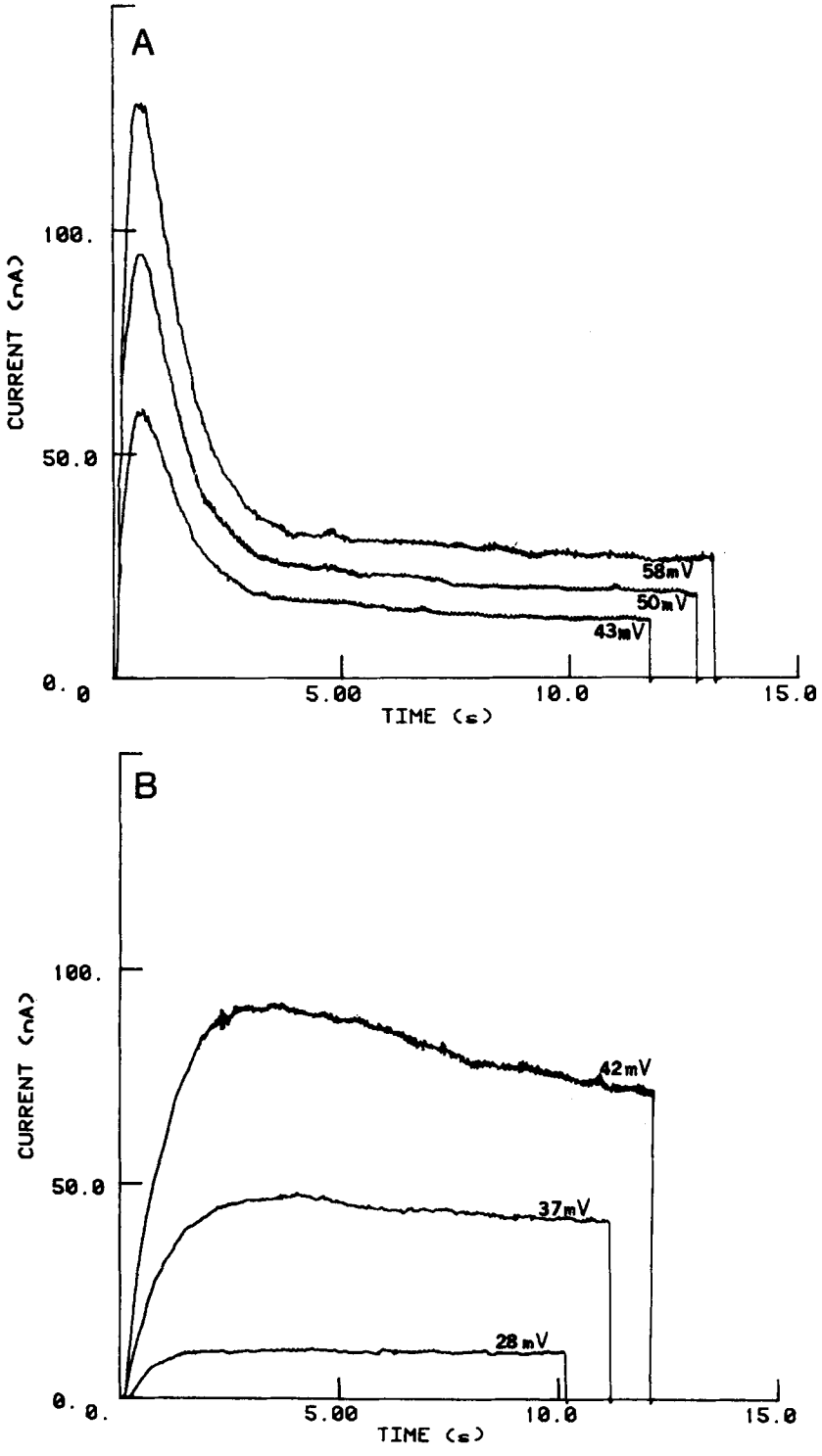
A
100.
50.0
0.0
CURRENT (nA)
58mV
50mV
43mV
0.0
5.00
10.0
15.0
TIME (s)
B
100.
50.0
0.0.
CURRENT (nA)
42mV
37mV
28mV
0.0.
5.00
10.0
15.0
TIME (s)

were measured in calcium free solution and μ_o and λ_o were adjusted to give the the appropriate kinetics.

The time-course of alamethicin kinetics *and the magnitude of the current* are well described by the model. It is particularly important to note that at comparable current densities, the measured surface potential, binding constant, and unstirred layer thickness give good agreement between model and experiment. The channel density in these experiments is on the order of 20 channels/μm^2 or a mean separation between channels of ~0.15 μm. Since the mean channel separation is much less than the unstirred layer thickness, the approximation that the calcium concentration depends only on the distance from the membrane is probably a good one.

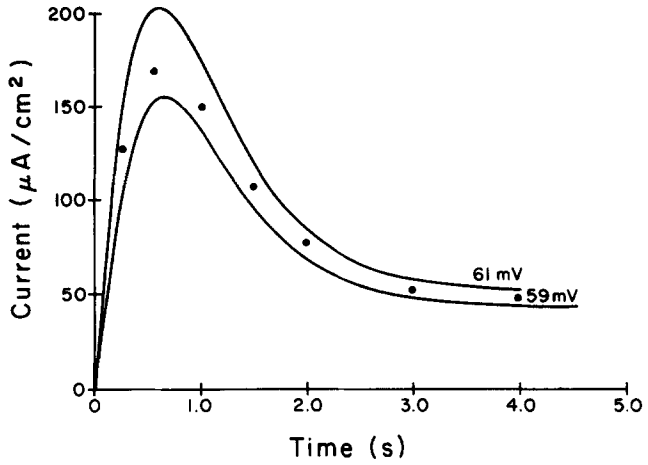

FIGURE 7. Comparison of alamethicin current response to a 58-mV voltage pulse in a membrane with a measured surface potential of 135 mV (●) with model calculations at 61 and 59 mV. Note that results agree very well with realistic values for the alterable parameters. The values for the unstirred layer thickness, the calcium concentration (13 mM), the surface charge (110 $Å^2$/electronic charge), and the calcium-PS binding constant (12 M^{-1}) are fixed. Only μ_0 and λ_0 are varied to obtain the fit. $\lambda_0 = 4.4 \times 10^6$ S^{-1}; $\mu_0 = 5.5 \times 10^{-19}$ A/(cm^2 S). $V_\mu = 6.9$ mV. $V_\mu = 10.0$ mV. Unstirred layer thickness = 100 μm.

Nickel acts in much the same way as calcium, inducing a flattening of the alamethicin current-voltage curve and inactivation of the current in response to a voltage pulse. We are unable to present a quantitative analysis at this time because the properties of alamethicin conductance in $NiCl_2$ have not been well studied.

Recovery from Inactivation: Effect of Unstirred Layer Thickness

For two voltage pulses of equal magnitude given in succession and separated by a variable delay time, the model predicts that the degree of recovery from inactivation depends only on the diffusion of calcium in the unstirred layer

and not on the alamethicin kinetic parameters. The time-course of the recovery depends on the thickness of the unstirred layer.

The peak currents of the recovery pulses shown in Fig. 8 A have a time constant of 6.9 s, and since $\tau/\delta^2 = 4/\pi^2 D = 8.11 \times 10^4$ cm^2/s. This value of τ gives an unstirred layer thickness of 86 μm, in good agreement with values estimated by other authors (Finkelstein, 1976). The curve in Fig. 8 A was

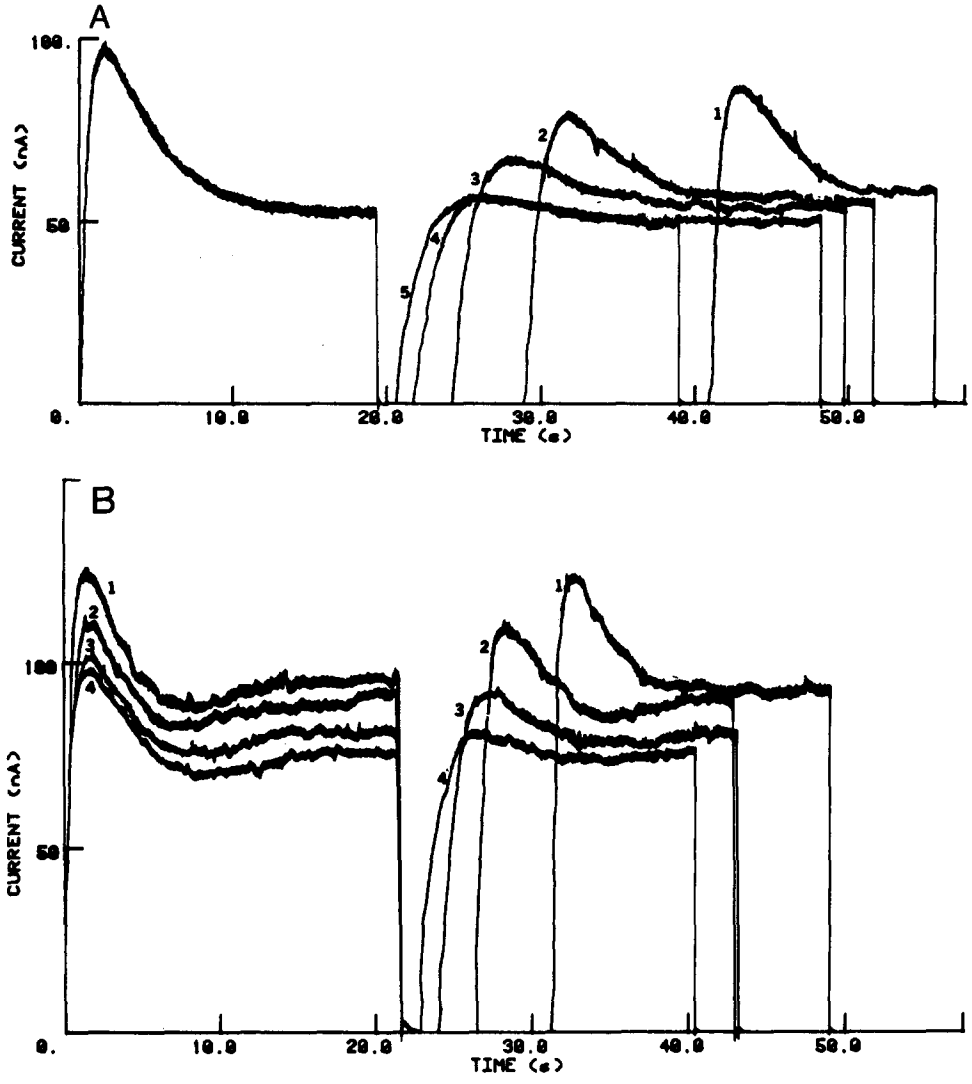

FIGURE 8. Recovery of the alamethicin conductance from calcium-induced inactivation without stirring (A). Between pulse pairs, the solutions were stirred vigorously with teflon coated magnetic stirring bars. In B, the membrane was stirred constantly. This reduces the time for recovery considerably (and adds increased noise because of membrane movement).

obtained with no stirring, but without allowing the solutions to rest for more than 30 s after previous stirring so the fluid undoubtedly still had a very large circulation, which would account for the finite value of the unstirred layer. Fig. 8 B shows a recovery curve obtained with very vigorous stirring. The time constant for recovery is ~2 s, corresponding to an unstirred layer thickness of 50 μm. Fig. 9 A and B shows computer simulations of recovery based on the model. The voltage pulse was 60 mV and the surface potential was ~55 mV in the simulations. These values correspond closely to the values in the

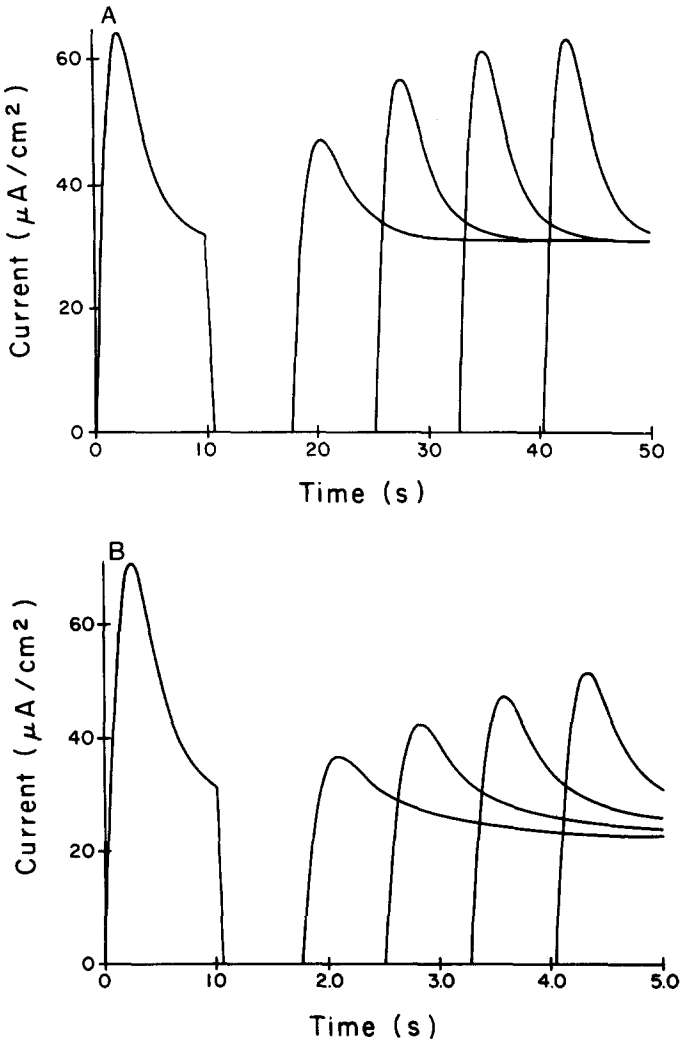

FIGURE 9. Computer simulations of recovery using parameters shown. In A, the unstirred layer thickness was 100 μm; in B, it was 200 μm. Note that the recovery is much slowed by a thick unstirred layer. $\lambda_0 = 4.4 \times 10^{-13}$ S^{-1}. $\mu_0 = 1.5 \times 10^{-10}$ A/(cm^2 S). $V_\mu = 6.9$ mV. $V_\lambda = 10.0$ mV.

experiment shown in Fig. 8 A. In the simulation in Fig. 9 A, the unstirred layer thickness was 100 μm. The only change in parameters in the simulation in Fig. 9 B is the alteration of the unstirred layer thickness to 200 μm. This alters the kinetics of both the recovery and the falling phase of the initial current response. Another effect of increasing the thickness of the unstirred layer is to decrease the current at steady state relative to the peak current. The physical reason for this, in terms of the model, is that the thicker the unstirred layer, the larger the calcium concentration at the surface of the membrane required to drive a diffusion flux across the unstirred layer equal to the flux across the membrane.

The stirred and unstirred recoveries show the qualitative differences expected from the model. The stirred recovery is faster than the unstirred and the stirred inactivation is less than unstirred inactivation, just as the model suggests.

The inactivation seen in the presence of calcium is not seen in the absence of calcium. It is thus not ascribable to asymmetric alamethicin concentrations, or to lipid flip-flop (Hall, 1981) and indeed occurs in essentially the same way with both symmetric and asymmetric alamethicin concentrations.

DISCUSSION

We have demonstrated that passage of the divalent cation, calcium, from the PE side of an asymmetric membrane to the PS side results in a substantial alteration of the surface potential and thus the voltage-dependent alamethicin conductance. A reasonable model fits the observed data well. Similar effects are observed in node of Ranvier from frog and as described in the companion paper (Cahalan and Hall, 1982), are qualitatively in agreement with the model. It is thus clear that the large alamethicin channel can pass enough calcium to make a very large difference in the surface potential of both planar bilayers and node of Ranvier. And, although naturally occurring calcium channels have much smaller conductances than alamethicin (Akaike et al., 1978), movement of calcium through these channels from the exterior of a cell to the interior could have a large effect on the local surface potential if certain conditions are met.

First, in our model, calcium that has passed to the PS side of the membrane is treated as diffusing away through the unstirred layer some 50–100 μm in thickness to an infinite sink. Making the unstirred layer *smaller* speeds up the attainment of steady state of calcium diffusion and thus speeds up surface potential change, but it reduces the magnitude of calcium-induced change. If, on the other hand, the perfectly absorbing plane at the edge of the unstirred layer were replaced by a perfectly reflecting plane, the attainment of steady state of the calcium response would become much faster *and* the effect of calcium would be much enhanced. Thus, if calcium were confined to a region near the inside of the cell membrane, either by mechanical barrier or an effectively lower diffusion coefficient, it would exert its effect on surface potential (assuming the inside of the cell membrane contained negative charges) more rapidly and more strongly than in the bilayer. It is conceivable

that cells have developed specialized mechanisms or structures for confining calcium to appropriate local regions of the membrane so that binding to surface sites to alter the effective membrane potential at those regions could act as a regulatory mechanism.

It is also possible that the model system we have demonstrated here may be of use in determining the extent to which such processes occur in biological membranes, a possibility more fully explored in the following paper.

We would like to thank T. Boles for technical assistance, Dr. I. Vodyanoy for helpful conversations, and Mary Ann Tacha and Karen Jessup for help in preparing the manuscript. The work was supported by National Institutes of Health grants NS 14609 and HL 23813, and Research Career Development Award HL 00579 to J. E. Hall.

Received for publication 30 November 1980 and in revised form 20 August 1981.

REFERENCES

AKAIKE, N., H. M. FISHMAN, K. S. LEE, L. E. MOORE, and A. M. BROWN. 1979. The units of calcium conduction in *Helix* neurones. *Nature (Lond.)*. **274**:379–381.

BEGENISICH, T. 1975. Magnitude and location of surface charges on *Myxicola* giant axons. *J. Gen. Physiol.* **66**:47–65.

BERRIDGE, M. J. 1975. Interactions of cyclic nucleotides and calcium in the control of cellular activity. *In* Advances in Cyclic Nucleotide Research, Vol. 6. P. Greengard and G. A. Robinson, editors. Raven Press, New York.

BOCKRIS, J. O'M., and A. K. N. REDDY. 1970. Modern Electrochemistry. Plenum Press, New York.

BOHEIM, G. 1974. Statistical analysis of alamethicin channels in black lipid membranes. *J. Membr. Biol.* **19**:277–303.

CAHALAN, M. D., and J. E. HALL. 1979. Node of Ranvier probed by alamethicin. *Biophys. J.* **25**:139*a*.

CAHALAN, M. D., and J. E. HALL. 1982. Alamethicin channels incorporated into frog node of Ranvier. Calcium-induced inactivation and membrane surface charges. *J. Gen. Physiol.* **79**:411–436.

EISENBERG, M., J. E. HALL, and C. A. MEAD. 1973. The nature of the voltage-dependent conductance induced by alamethicin. *J. Membr. Biol.* **14**:143–176.

FINKELSTEIN, A. 1976. Water and nonelectrolyte permeability of lipid bilayer membranes. *J. Gen. Physiol.* **68**:127–135.

GILBERT, D. L., and G. EHRENSTEIN. 1969. Effect of divalent cations on potassium conductance of squid axons: determination of surface charge. *Biophys. J.* **9**:447–463.

GINSBERG, B. L., and C. R. HOUSE. 1980. Stimulus-response coupling in gland cells. *Annu. Rev. Biophys. Bioeng.* **9**:55–80.

GORDON, L. G. M., and D. HAYDON. 1972. The unit conductance channel of alamethicin. *Biochim. Biophys. Acta.* **255**:1014–1018.

HALL, J. E. 1981. Voltage-dependent lipid flip-flop induced by alamethicin. *Biophys. J.* **33**:373–381.

HALL, J. E., and R. LATORRE. 1976. Nonactin-K^+ complex as a probe for membrane asymmetry. *Biophys. J.* **15**:99–103.

HILLE, B., A. WOODHULL, and B. SHAPIRO. 1975. Negative surface charge near sodium channels

of nerve: divalent ions, monovalent ions, and pH. *Phil. Trans. R. Soc. Lond. B. Biol. Sci.* **270**:301–318.

HUBBELL, W. L., and M. D. BOWNDS. 1979. Transduction in vertebrate photoreceptors. *Annu. Rev. Neuro. Sci.* **2**:17–34.

KELLY, R. B., J. W. DEUTCH, S. S. CARLSON, and J. A. WAGNER. 1979. Biochemistry of neurotransmitter release. *Annu. Rev. Neuro. Sci.* **2**:399–446.

MATHEWS, J., and R. L. WALKER. 1965. Mathematical Methods of Physics. W. A. Benjamin, Inc., New York.

MCLAUGHLIN, S., N. MULRINE, T. GRESALFI, G. VAIO, and A. MCLAUGHLIN. 1981. The adsorption of divalent cations to bilayer membranes containing phosphatidyl serine. *J. Gen. Physiol.* **77**:445–475.

MCLAUGHLIN, S. G. A., G. SZABO, G. EISENMAN, and S. CIANI. 1970. Surface charge and the conductance of phospholipid membranes. *Proc. Natl. Acad. Sci. U. S. A.* **67**:1268–1275.

MEECH, R. W. 1978. Calcium-dependent potassium activation in nervous tissues. *Annu. Rev. Biophys. Bioeng.* L. J. Mullins, editor. Annual Review, Inc., Palo Alto, California.

MONTAL, M., and P. MUELLER. 1972. Formation of bimolecular membranes from lipid monolayers and a study of their properties. *Proc. Natl. Acad. Sci. U. S. A.* **69**:3561.

SCHINDLER, H.-G., and G. FEHER. 1976. Branched bimolecular lipid membranes. *Biophys. J.* **16**:1109–1113.